

## **7. Temporal Changes in Meteorology, Transport, and Air Quality**

This section compares the Project MOHAVE study year to other years in terms of meteorology and air quality and describes seasonal and yearly variations in transport patterns.

### **7.1 Representativeness of Meteorology and Air Quality**

#### **7.1.1 Meteorology**

The Grand Canyon Visibility Transport Commission evaluated calendar year 1992 for climatological representativeness for the 15-year period from 1977-1982 and 1984-1992 (Farber, 1995). This 15-year period, which is half the accepted climatological base period of 30 years, was dictated by the availability of visibility and aerosol data in the area. The calendar year was divided into two meteorological seasons: winter, January-April and November-December; and summer, the remaining months (May-October). To determine representativeness of each season, a chi-squared analysis was performed and then each season was comparatively ranked.

This analysis determined that 1992 was a "typical" year and that both winter and summer were "typical" seasons in a mix of "atypical" years and seasons. The 15 years examined had wide inter-annual variability among each season and both winter and summer of 1992 were not out of this wide variability range.

Winters exhibit less inter-annual variability than summers. The chi-squared summation value for the 15 winter seasons was 166 compared to 229 for the 15 summer seasons. This result may seem unexpected. One might expect greater variability during winter because of alternating storm and fair weather patterns compared to essentially fair weather patterns during summer. However, during winter, patterns are more strongly defined, more predictable (dominated by fair weather patterns) and surprisingly, do not reflect too much variation in the interannual variability of the storm pattern. By contrast, summers have less clearly separated patterns and, because of the intrinsic fuzziness of the two dominant patterns, the "thermal low" and "monsoonal", have greater inter-annual seasonal variability.

1992 was a moderate El Niño year in the southwestern United States, which led to above normal precipitation and clouds, particularly during the winter season. The chi-squared value for the winter of 1992 was about 20 compared to a seasonal average of 11. Most of this high value emanated from atypically high "thermal low" patterns (strong westerlies in the desert southwest) which occurred nearly 40% of the winter compared to the climatological average of 25%.

The summer was more climatologically normal than the winter. The 1992 summer season chi-squared value was 15 compared to the climatological average of 20. There are some important caveats. Summer 1992 (May-Oct) had the lowest number of troughs and the fourth highest number of monsoonal patterns for the 15 years examined. The heart of the summer was characterized by a strong and persistent high with above normal precipitation and accompanying clouds. This is typical of an El Niño year because there is more than the usual amount of sub-tropical moisture flowing into the region.

### 7.1.2 Light Extinction

Transmissometer-measured light extinction in 1992 at the south rim of the Grand Canyon and in the canyon were compared to the years 1987-1994. Generally, the 1992 year and summer and winter seasons were representative of the observed range of extinction. The annual median extinction at Grand Canyon ranged from 21 to 23  $\text{Mm}^{-1}$  with 1992 recording a representative 22  $\text{Mm}^{-1}$ . The summer seasonal median extinction on the rim ranged from 21 to 27  $\text{Mm}^{-1}$  with 1992 recording 24  $\text{Mm}^{-1}$ . Within the Canyon, summer median extinction ranged from 30-36  $\text{Mm}^{-1}$  with 1992 recording 32  $\text{Mm}^{-1}$ . The winter seasonal median ranged from 17 to 20  $\text{Mm}^{-1}$  on the rim with 1992 recording 19  $\text{Mm}^{-1}$ . Within the canyon the median ranged from 25 to 33  $\text{Mm}^{-1}$  with 1992 being at the high end, 33  $\text{Mm}^{-1}$ .

The entire frequency distribution (Figure 7-1 through Figure 7-4) from 10<sup>th</sup> through 90<sup>th</sup> percentile was also examined. For the summer, both on the rim and in-canyon 1992 was typical of the longer term average through the 50<sup>th</sup> percentile. However, from the 60<sup>th</sup> through 90<sup>th</sup> percentile, 1992 was nearly the clearest summer year. For example, at the 90<sup>th</sup> percentile, extinction in the Canyon ranged from 40 to 46  $\text{Mm}^{-1}$  with 1992 being 40  $\text{Mm}^{-1}$ .

On the rim, winter was slightly hazier than average until the 90<sup>th</sup> percentile, where it was average. In the canyon, the 1992 winter was hazier than average throughout the distribution. As expected, winter experiences the lowest extinction on the rim. This should not be surprising given that, more than 80% of the time, winter trajectories have a relatively clear northerly origin. In surprising contrast to the clear plateaus during winter, winter extinction in the canyon is actually higher than summer extinction on the rim throughout all percentiles. This is due to winter mesoscale drainage flows throughout the Colorado Plateau. These large scale drainage flows dominate for 18 hours daily during fair weather periods. A variety of anthropogenic sources from eastern Utah, western Colorado, northern Arizona and northwestern New Mexico feed into this extensive drainage system. Somewhat surprisingly, even during summer, when the atmosphere is well-mixed, there is still appreciably higher extinction in the canyon compared to the rim. Nocturnal drainage flows still occur most summer nights (see Section 5.3).

### 7.1.3 Sulfate

Particulate sulfate concentrations at both Meadview and Hopi Point were examined. The concentrations were representative at both locations compared to other years.

At Meadview, SCENES data collected from 1984 through 1989 were compared to the Project MOHAVE data. All values are expressed in particulate S. For the entire year, the SCENES 50<sup>th</sup> percentile was 0.37  $\text{ug/m}^3$  compared to the Project MOHAVE year of 0.36  $\text{ug/m}^3$ . Between the 10<sup>th</sup> and 90<sup>th</sup> percentiles, the two studies are quite comparable with not more than 0.03  $\text{ug/m}^3$  separating the two studies at any percentile.

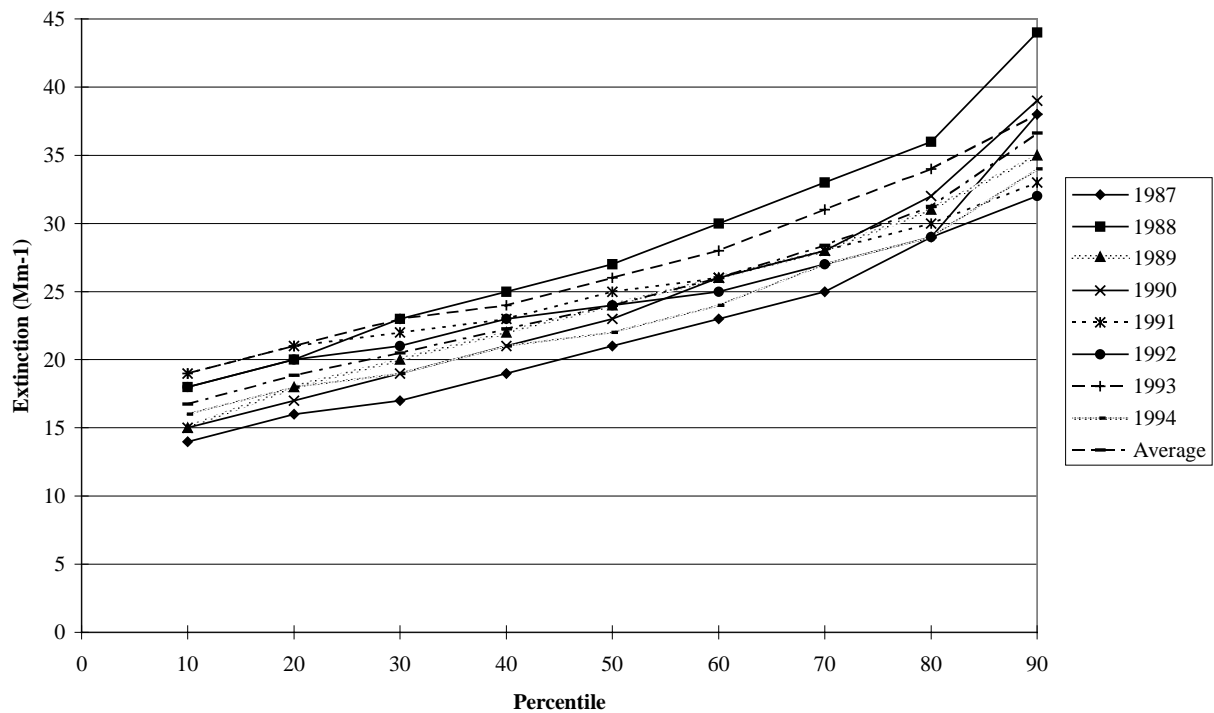


Figure 7-1 Frequency distribution of light extinction at Grand Canyon by season and year: south rim, summer (May – October).

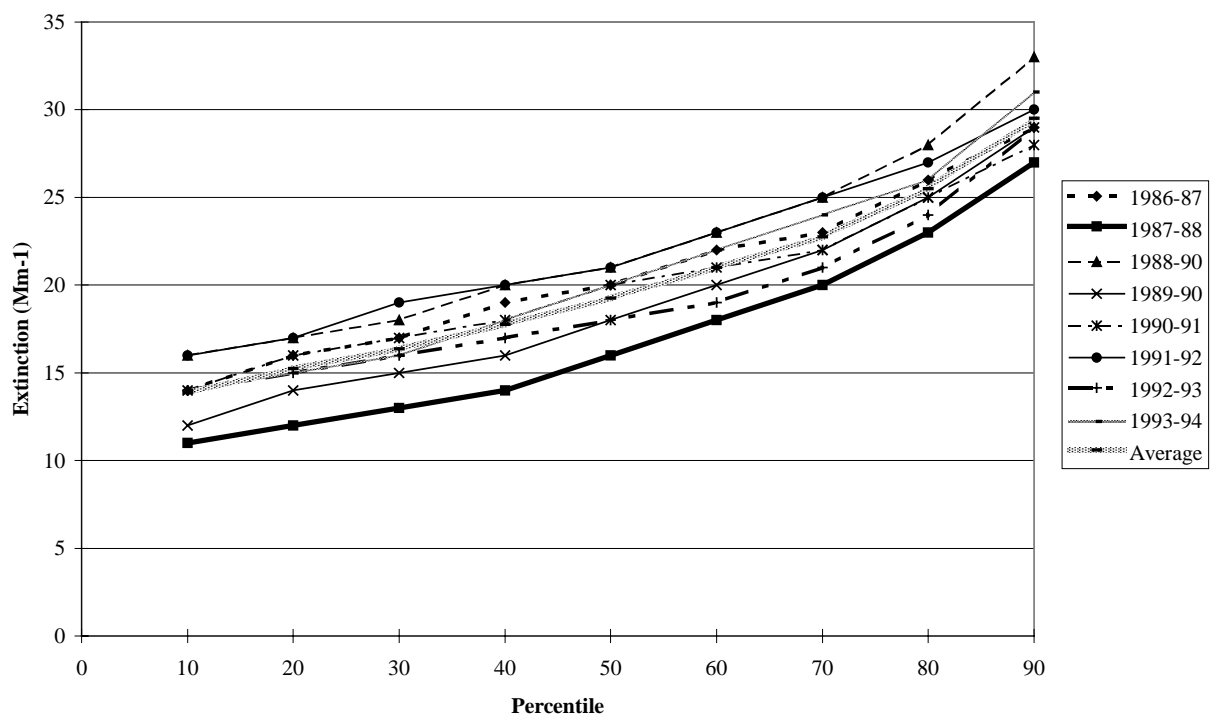


Figure 7-2 Frequency distribution of light extinction at Grand Canyon by season and year: south rim, winter (November – April).

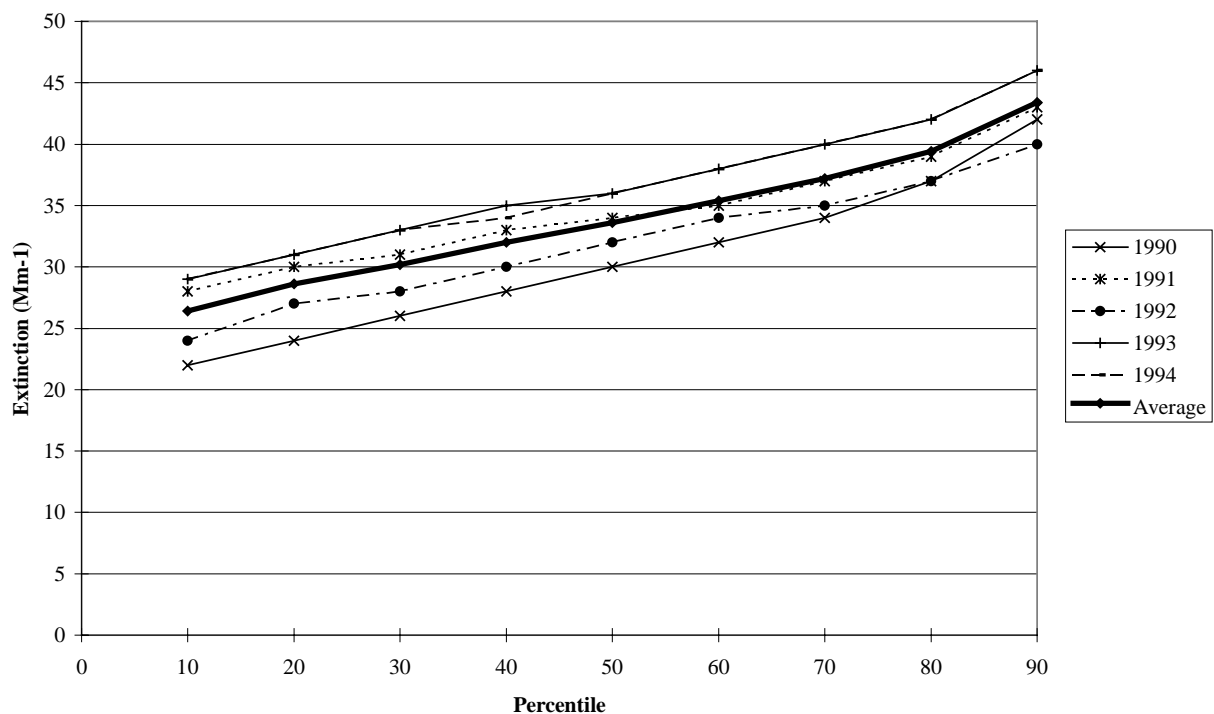


Figure 7-3 Frequency distribution of light extinction at Grand Canyon by season and year: incanyon, summer (May – October).

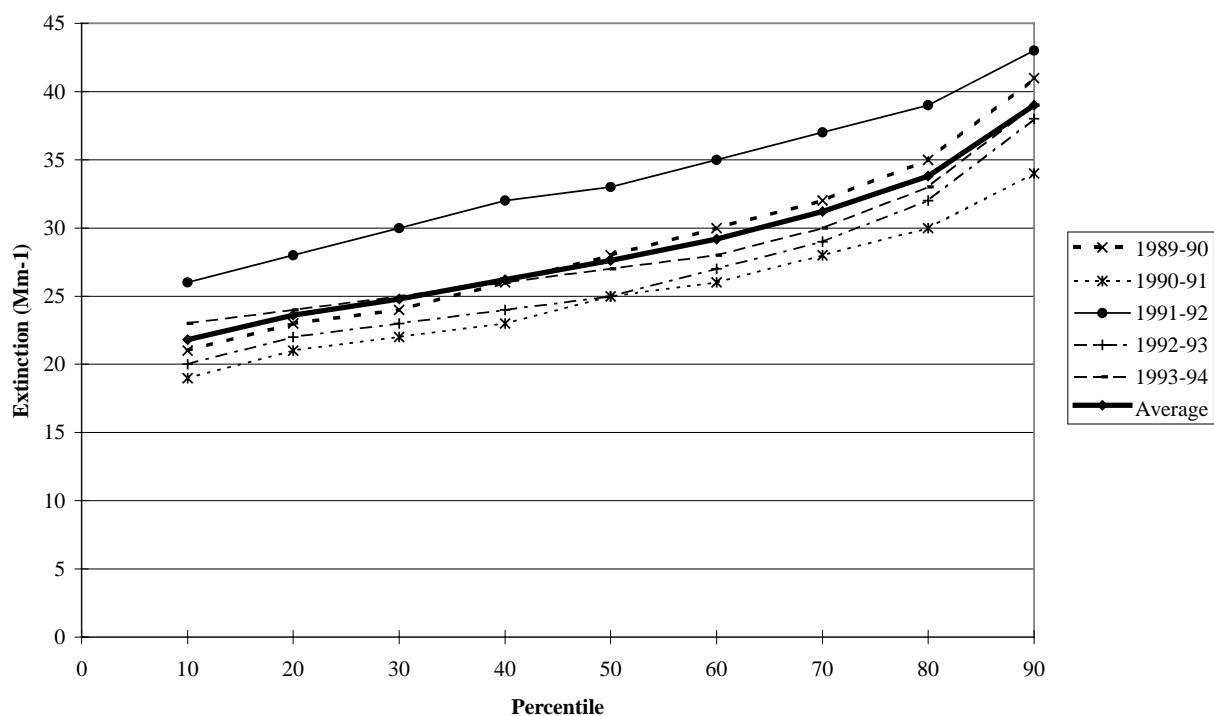


Figure 7-4 Frequency distribution of light extinction at Grand Canyon by season and year: incanyon, winter (November – April).

For the summer, (May-September), the 50<sup>th</sup> percentile at Meadview during SCENES was 0.44  $\mu\text{g}/\text{m}^3$  compared to 0.51  $\mu\text{g}/\text{m}^3$  during the 1992 Project MOHAVE summer (see Figure 7-5 and Figure 7-6). Below the 50<sup>th</sup> percentile, the Project MOHAVE summer was approximately 0.06  $\mu\text{g}/\text{m}^3$  higher, perhaps a result of the absence of "cleaner" troughs and more monsoonal periods and high pressure periods during 1992. Above the 50<sup>th</sup> percentile, the concentrations between the two studies were very similar. For the summer intensive monitoring period (July 12 through August 31), the SCENES 50<sup>th</sup> percentile was 0.50  $\mu\text{g}/\text{m}^3$  compared to 0.53  $\mu\text{g}/\text{m}^3$  for Project MOHAVE. Below the 50<sup>th</sup> percentile, the Project MOHAVE summer intensive period was approximately 0.03 to 0.05  $\mu\text{g}/\text{m}^3$  higher than the SCENES period. Above the 50<sup>th</sup> percentile, the SCENES period was higher by about 0.03  $\mu\text{g}/\text{m}^3$ . (It should be noted that SCENES and Project MOHAVE used different sampling techniques, which may result in some systematic differences.)

For the period corresponding to the winter intensive monitoring period (January 14-February 13), the SCENES 50<sup>th</sup> percentile was 0.22  $\mu\text{g}/\text{m}^3$  compared to Project MOHAVE 0.19  $\mu\text{g}/\text{m}^3$ . The SCENES winter intensive period had consistently higher S concentrations from the 10<sup>th</sup> through the 90<sup>th</sup> percentile by as much as 0.1  $\mu\text{g}/\text{m}^3$  at the higher end.

At Hopi Point, the data record is longer than at Meadview and contains data from even before the 1984 start of SCENES through the present. Here the Project MOHAVE period is compared to SCENES (1984-1989) and IMPROVE (1987 through Sept 1997). Particulate S concentrations showed a downward trend in the higher percentiles from 1984 through Sept 1997. For the entire Project MOHAVE year, the 50<sup>th</sup> percentile was 0.29  $\mu\text{g}/\text{m}^3$  compared to SCENES 50<sup>th</sup> percentile of 0.27  $\mu\text{g}/\text{m}^3$  and IMPROVE 50<sup>th</sup> percentile of 0.22  $\mu\text{g}/\text{m}^3$ . SCENES is higher than IMPROVE for all percentiles by approximately 0.02  $\mu\text{g}/\text{m}^3$  at the low end to 0.11  $\mu\text{g}/\text{m}^3$  at the high end. Project MOHAVE is between these two sets of data. The Project MOHAVE and SCENES summer medians were identical at 0.34  $\mu\text{g}/\text{m}^3$  compared to IMPROVE 0.30  $\mu\text{g}/\text{m}^3$ . The Project MOHAVE summer intensive study median was 0.38  $\mu\text{g}/\text{m}^3$  compared to SCENES 0.40  $\mu\text{g}/\text{m}^3$  and IMPROVE 0.30  $\mu\text{g}/\text{m}^3$  (see Figure 7-6).

## **7.2 Transport Patterns**

An overview of synoptic scale and mesoscale meteorology affecting the study area was given in section 2.2. In this section, trajectory analyses and other information are presented to describe how the seasonal and year-to-year variations in meteorology affect transport to the Grand Canyon.

### **7.2.1 Seasonal synoptic scale transport patterns**

Typical synoptic-scale patterns can be seen by back-trajectory analyses. ATAD (Atmospheric Transport and Dispersion) back-trajectories were run for Hopi Point for the period 1979-1992, 4 trajectories per day. In brief, the ATAD model is a Lagrangian particle model with a single variable depth transport layer, the depth of which is determined by atmospheric stability using interpolation of measured vertical temperature profiles. Average transport layer winds are interpolated spatially and temporally from nearby radiosonde stations (Heffter, 1980). These trajectories were grouped by ½ month periods. The annual cycle of transport patterns can be

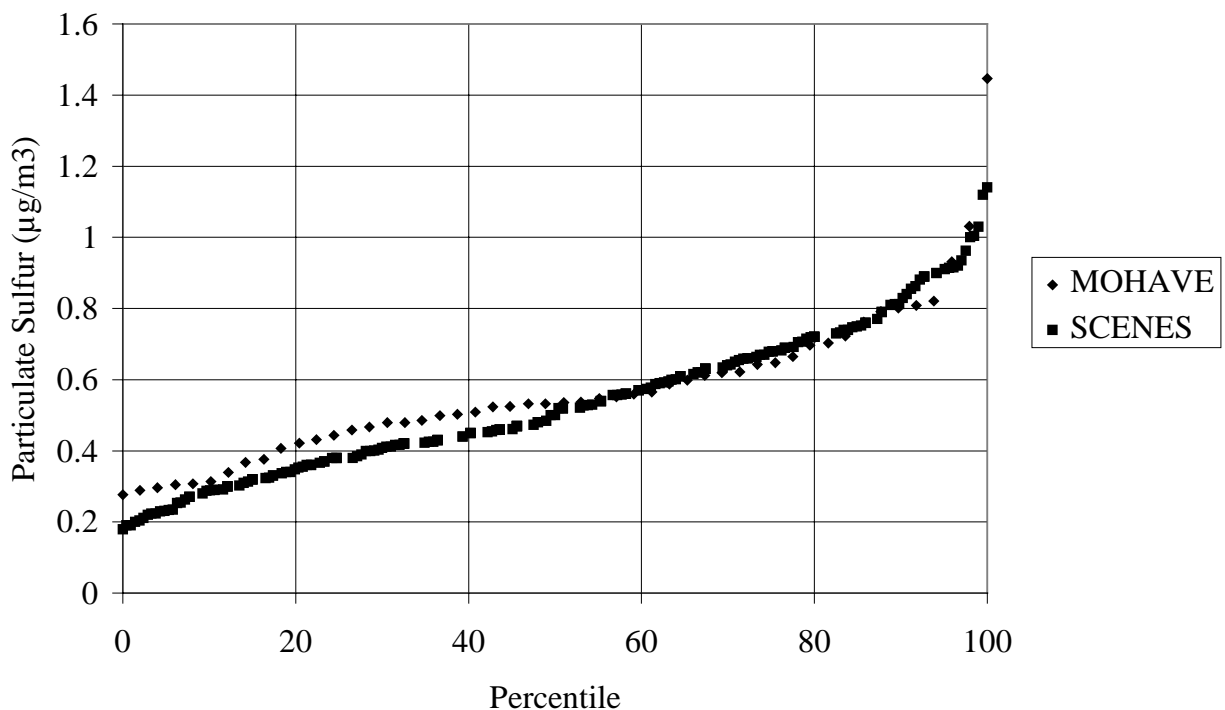


Figure 7-5 Frequency distribution of particulate sulfur at Meadview for the MOHAVE summer intensive period (July 13 – September 2) compared to the same period for SCENES.

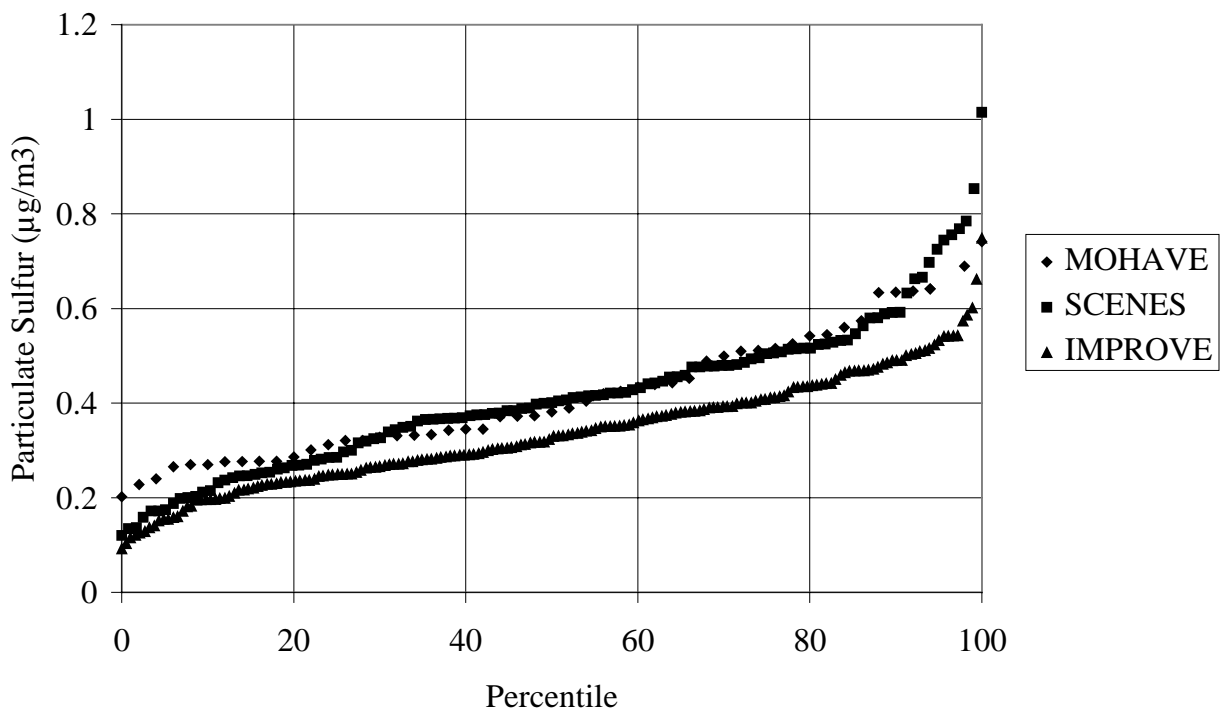


Figure 7-6 Frequency distribution of particulate sulfur at Hopi Point for the MOHAVE summer intensive period (July 13 – September 2) compared to the same period for SCENES (1984-1989) and IMPROVE (1987-1997).

discerned by looking at 6 specific half-month periods. Figure 7-7 shows the fraction of back-trajectories passing over grid cells of 2 degrees latitude by 2 degrees longitude for these 6 half-month periods. Northwestern flow is common in late-fall and winter and the frequency peaks in late November (Figure 7-7). In mid-winter no direction dominates the synoptic scale transport pattern (Figure 7-7b). During this time low-pressure systems frequently pass through the region, resulting in a variety of wind directions as the pressure gradient direction and hence wind direction changes as the systems approach and pass through the area. In spring a transition period occurs between the northwesterly flow common in winter to the dominant southwesterly flow in the summer. In late April (Figure 7-7c), a bi-modal distribution of southwesterlies and northwesterlies is observed. Late June marks the peak of the frequency of transport from the southwest (Figure 7-7d). By mid-late summer, flows from the southeast (accompanied by considerable moisture) are more frequent (Figure 7-7e). Finally, in late September, transition to northwesterlies is beginning, although southwesterly and southeasterly patterns are still significant (Figure 7-7f).

## 7.2.2 Effect of transport patterns upon haze levels

Several analyses (e.g. Kahl *et al.*, 1997, Green and Gebhart, 1997, Vascancelos, 1997, Gebhart and Green, 1995, White *et al.*, 1994a, Gebhart and Malm, 1994) have been performed in the last few years that consider the relationship between transport patterns and air quality at Grand Canyon National Park. These analyses used aerosol and optical data from either the SCENES network (1984-1989) or the IMPROVE network (late 1980's to early 1990's). The conclusions are consistent among the different analyses and include:

- Clear (low  $b_{\text{ext}}$ ) air most commonly arrives during winter and from the northwest.
- Hazy (high  $b_{\text{ext}}$ ) air most commonly arrives during summer and from the southwest; air arriving from the southeast, mainly in summer is also dirty, but less frequent.
- Most particulate sulfur transported to the Grand Canyon is from the southwest; however, average concentrations of fine sulfur are highest with transport from the southeast.
- Transport from the northwest has the lowest average particulate sulfur concentrations.

Figure 7-8 (Green and Gebhart, 1997) shows the probability that air arriving at Grand Canyon with trajectories passing over each grid cell had light extinction coefficients at Grand Canyon in the lowest 20 percentile for the period 1988-1992. Trajectories from the north were likely to be associated with low  $b_{\text{ext}}$ , while trajectories from the south were unlikely to be associated with low  $b_{\text{ext}}$ .

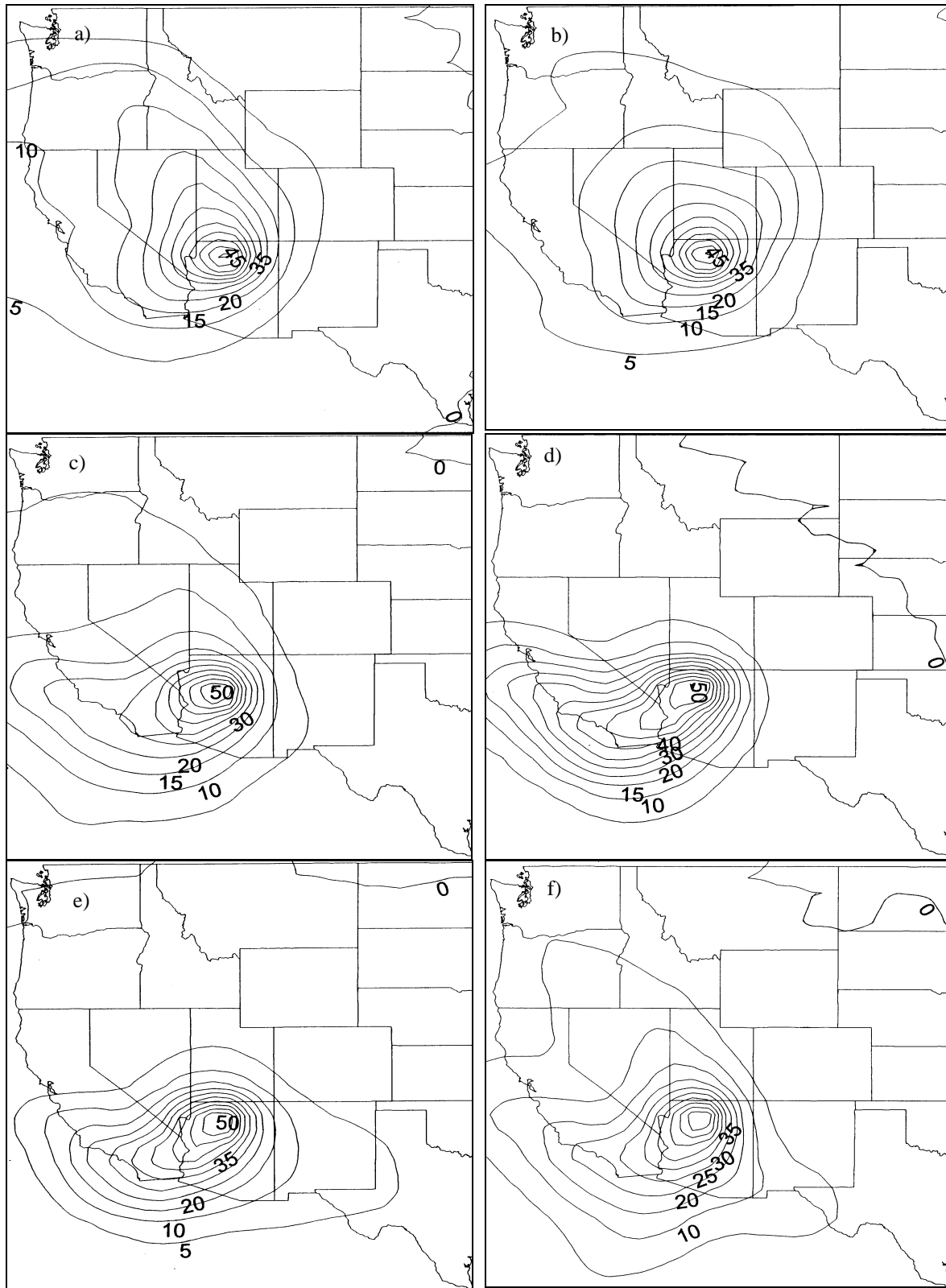


*Figure 7-7 Percent of trajectories passing over 2 degree longitude by 2 degree latitude grid cells en route to Grand Canyon, 1979-1992. a) Nov. 16-30; b) Jan. 1-15; c) Apr. 15-30; d) June 15-30; e) August 1-15; f) Sep. 15-30.*



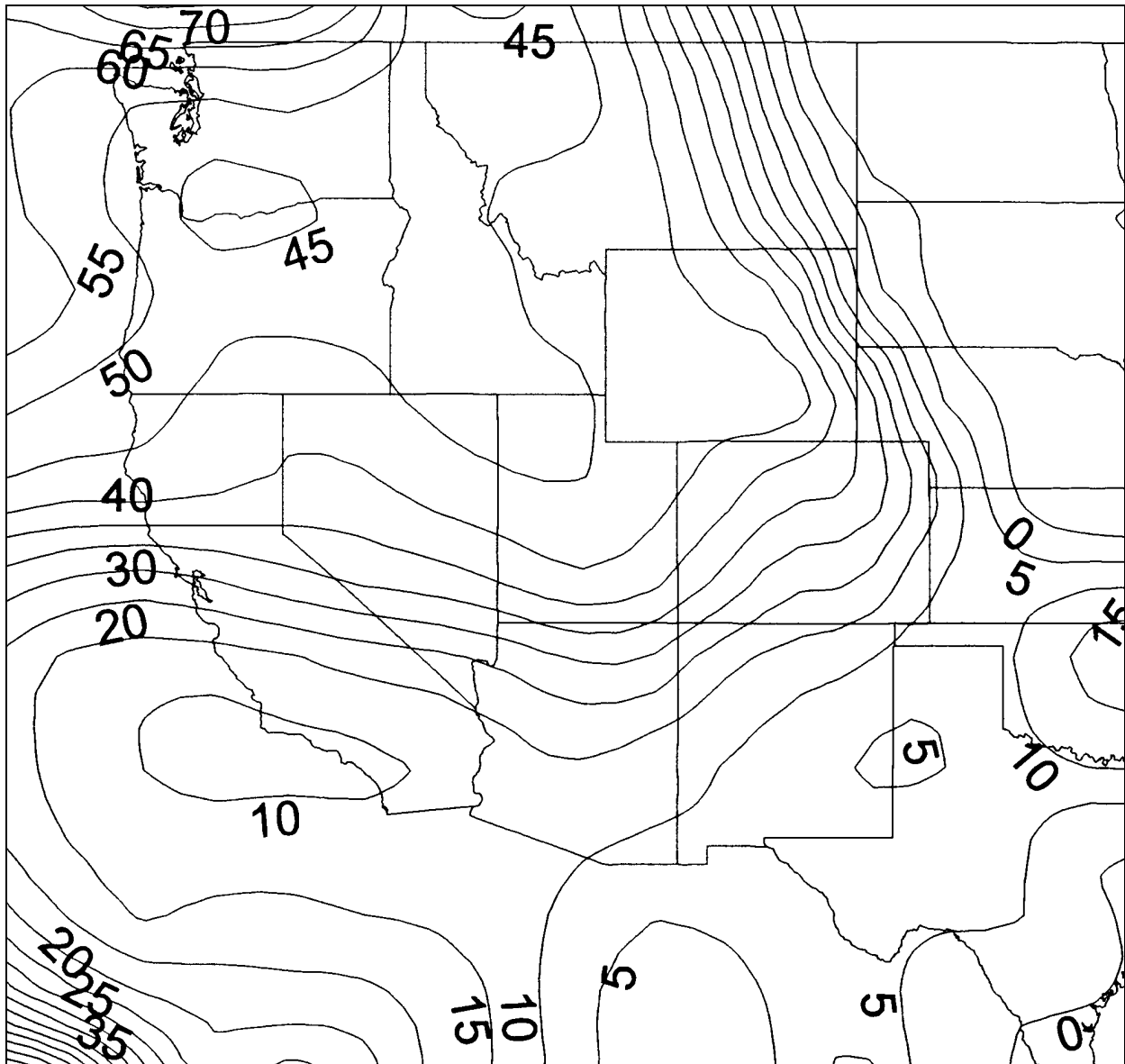


Figure 7-8 Probability that air arrived at Grand Canyon with low light extinction (lowest 20<sup>th</sup> percentile) after passing over each area, according to ATAD trajectories, 1988-1992.

### 7.2.3 Mesoscale transport patterns

Project MOHAVE tracer data provides quantitative and qualitative information about transport and dispersion in the study area. While the tracer data showed some variation from day to day within the summer and winter periods, typical patterns did emerge. Figure 7-9 shows the frequency of samples significantly above background concentrations during the PFT release periods for sites in the winter intensive that collected at least 20 days of samples, and for sites in the summer intensive period that collected at least 30 days of samples. A sample is considered to be significantly above background if its concentration is greater than the background plus 3 standard deviations of the measured background concentration. Shaded contour patterns are

included to guide the viewers to sites of similar frequency and should not be literally interpreted as spatial patterns.

Figure 7-9c shows Dangling Rope tracer in winter was most often transported to sites to the southwest, with even higher frequency for sites in or near the Colorado River Canyon. MPP tracer in winter was transported most frequently to sites to the south (Figure 7-9a). The Dangling Rope PFT data are above background concentrations in greater than 40% of the samples along the Colorado River through the entire length of the Grand Canyon and in more than 20% of the samples as far down river as MPP. Unfortunately, there were only a few sites south of MPP with sufficient data to track the MPP tracer flow very far. However winter flow is not exclusively downslope as shown by small, but non-zero, frequency for PFT above background concentrations to the north of MPP for its PFT and to the northwest of Dangling Rope for its PFT.

In the summer, the MPP PFT is above background levels most of the time at sites north of MPP, which indicates a northerly predominant direction of flow (Figure 7-9b). At San Geronio, 66% of the samples were determined to be above background for the MPP PFT: most of these samples were from one lid and many were only marginally above background. This suggests a possible analytical problem, for example variation in response of the gas chromatograph, rather than actual elevated concentrations of ocPDCH. Alternatively it is possible that a small source of ocPDCH or compounds that are analyzed as ocPDCH (interferences) are present in the greater Los Angeles area.

PFT from El Centro in summer is also seen most frequently at sites to the north (Figure 7-9e). From the Tehachapi location the flow tends to be toward sites to the east (Figure 7-9d). Lack of monitoring sites to the north of the Tehachapi Pass PFT release site prevents conclusions concerning travel in that direction, though it is clear that flow does not frequently carry that tracer to sites to the southeast.

#### **7.2.4 Influence Functions**

Figure 7-10 shows maps displaying mean influence functions for the PFT tracers. Influence functions are the emission rate normalized PFT concentrations (i.e. tracer concentration divided by emission rate) and have units of seconds/cubic meter. This convention readily permits the estimation of the contribution of a particular source to the atmospheric concentration (in  $\mu\text{g}/\text{m}^3$ ) at a receptor by multiplication of the influence function by the emission rate (in  $\mu\text{g}/\text{s}$ ) of the source. Values shown in Figure 7-10 have been multiplied by  $10^{-9}$  and contour intervals are in logarithmically distributed intervals. In order to reduce the uncertainty of the influence functions, periods of constant tracer emission were selected such that the average daily emission rate did not differ by more than 20% from the mean daily emission rate for the period. Since Dangling Rope, El Centro, and Tehachapi were located at the perimeter of the sampling network, influence functions were not calculated for the first two days of a constant emission period. This was assumed to be a sufficient time for the tracer to reach all of the sites within the network. Since the Mohave Power Project was centrally located in the network, influence functions were not calculated on the first day of each period. At least 20 days of influence functions at each site were required for the average to be plotted on the maps.

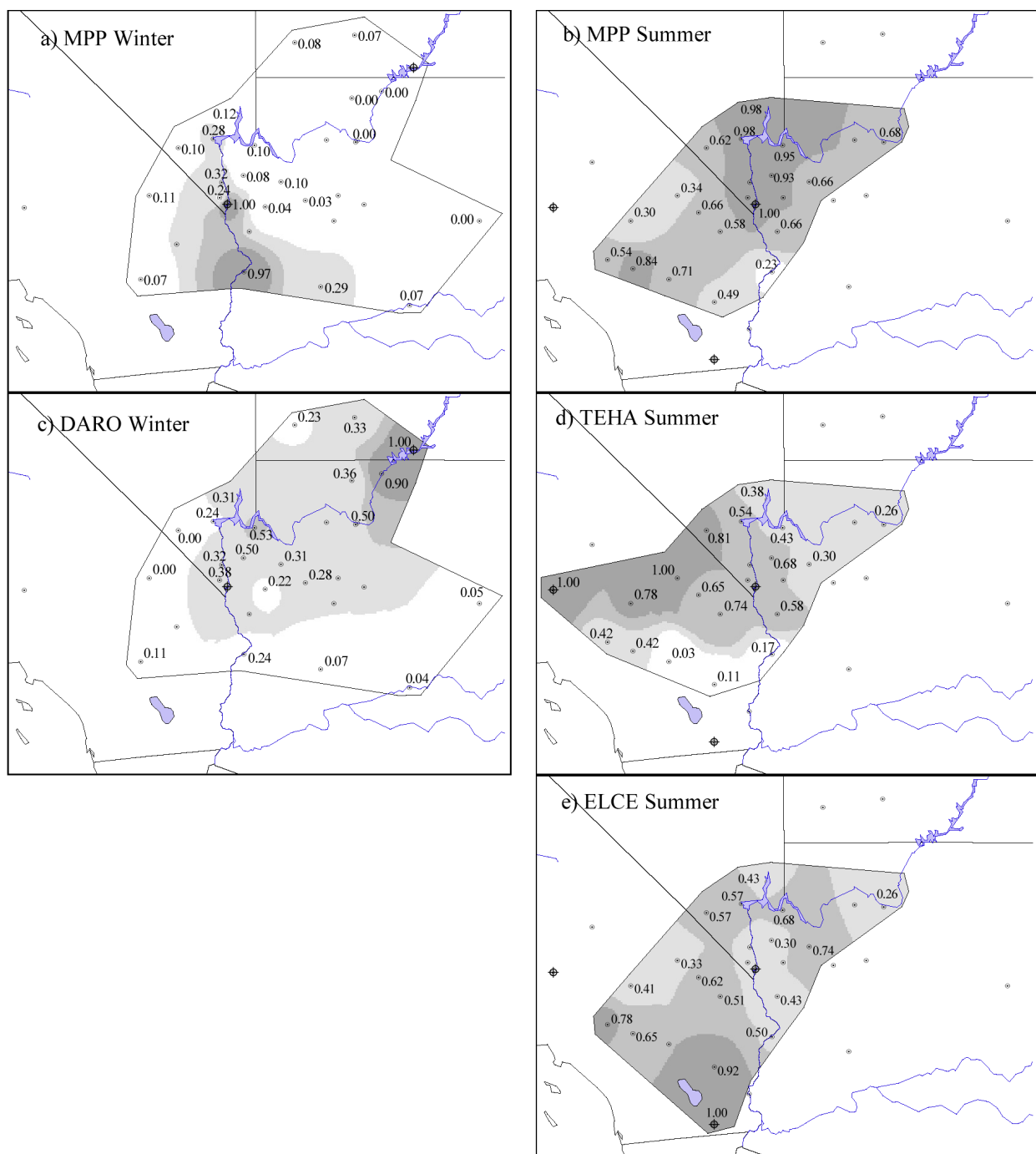


Figure 7-9 Maps of the frequency that tracer was detected above background for each of the four PFT release locations. Only data meeting completeness criteria were used to generate the contours. The polygons surround the sites meeting the completeness criteria.

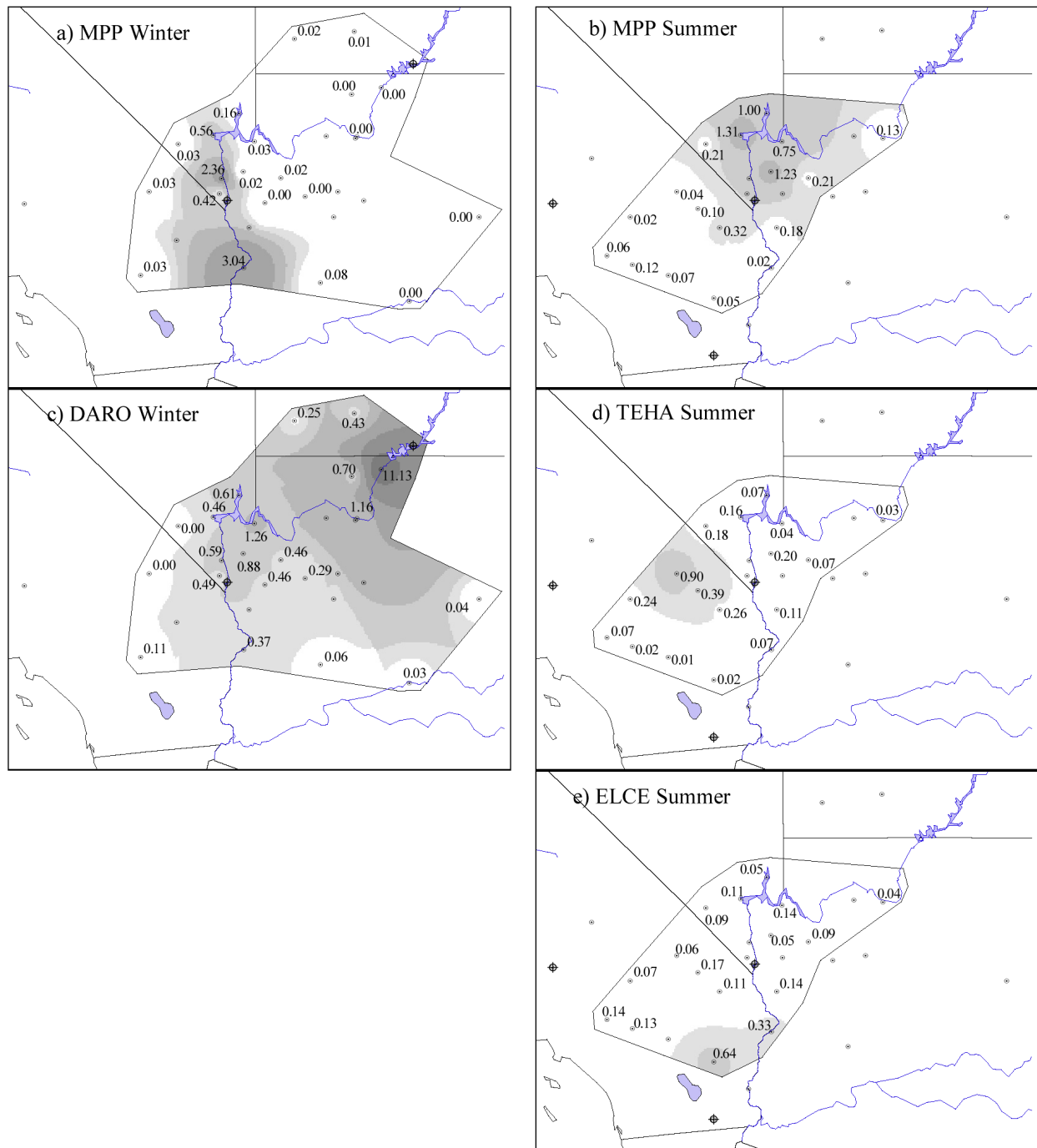


Figure 7-10 Map of average PFT influence functions ( $10^{-9} \text{ s/m}^3$ ) measured at receptor sites.

Influence functions are a direct measure of the average dispersion between the emission and monitoring locations. The spatial patterns of the mean influence functions illustrate the typical tracer distribution observed throughout each season. As might be expected, the largest values on the maps in Figure 7-10 are during the winter intensive period, and these tend to be at sites along the Colorado River canyon which acts as a natural conduit for airflow in the winter. The effect in winter of monitoring site height above local terrain can be seen in the Dangling Rope average influence functions for Hopi Point (situated on high local terrain) and Meadview (at mid-level

with respect to local terrain). The influence function is somewhat higher at Meadview than at Hopi Point in spite of the former being more than twice the distance from Dangling Rope than the latter. Winter flow for MPP also follows the Colorado River with the greatest influence function values to the south at Parker. Summer MPP average influence function values are highest at sites to the north with the largest average value at Las Vegas Wash. Tehachapi Pass average influence functions are largest in the northeastern Mojave Desert, while for El Centro the sites to the north (Desert Center and Parker) and northwest (Joshua Tree) of the release site have the largest average values. A predominant feature of winter flow shown by the PFT data is drainage down the Colorado River. Under these circumstances the dispersion is retarded by confinement within the terrain as can be seen with the high average influence functions at large distances downwind. Sources on the Colorado River east of the Grand Canyon, as represented by the Dangling Rope PFT, can have significant influence throughout the entire length of the Grand Canyon and beyond. MPP emissions are transported primarily to the south along the river and are soon beyond the few sites in the Project MOHAVE network to the south of MPP. While the direction of the flow was expected, the magnitude of the influence functions for the Dangling Rope release were surprisingly large at the more distant sites on the lower Colorado River. Neither of the two earlier winter studies that released tracer from near that location (WHITEX and the NGS Visibility Study) had tracer monitoring sites as far downriver as in Project MOHAVE.

Summer flow is generally from the south along the Colorado River (El Centro and MPP) and from the west (or possible southwest) from the western edge of the Mojave Desert (Figure 7-10 b and e). However, from the joint El Centro - Tehachapi frequency plots (not shown here) there appears to be a convergence zone over much of the Mojave Desert. PFTs from both of the two California release locations are above background in 20% to 30% of the 24-hour periods at all of the eastern Mojave Desert sites. Given that the flows from the greater Los Angeles and San Diego urban areas are likely to be located between the paths taken by the two PFTs, emissions from these areas must be at least as frequently transported through this region. This is consistent with predominate summer surface wind flow patterns for California, which have transport from the California Central Valley south-southeast over Tehachapi Pass, transport from the California South Coast Air Basin to the east into the Mojave Desert and flow to the north over the eastern half of the California - Mexico border. Convergence over the Mojave Desert can be explained by the thermally induced low pressure often centered over that area in summer which draws cooler air in from the California Central Valley, Pacific Coast and the Gulf of California. From this it is reasonable to conclude that the eastern Mojave Desert is a major transport route for emissions from much of the State of California during the summer.

The average summer MPP influence function values at Las Vegas Wash and Overton Beach are comparable to the average value at Dolan Springs in spite of the former being more than twice the distance from MPP. This suggests that MPP emissions are consistently over most of Lake Mead (north of MPP along the Colorado River) with relatively little dilution. An examination of the spatial MPP PFT influence function patterns for sample periods that have the highest influence functions at Meadview (where Lake Mead meets Grand Canyon) show that they are associated with flow passing over the Dolan Springs site to the east of MPP and not in the Colorado River canyon. This would seem to imply the need for a more westerly component to the wind to produce the largest MPP PFT concentrations in the western Grand Canyon.

### 7.3 Effect of Sulfur Dioxide Emissions Reductions on Sulfate Concentrations in the Western U.S. since 1979

Sulfur dioxide emissions in the Southwest have declined substantially in the past two and a half decades. As Figure 7-11 shows, SO<sub>2</sub> emissions in 5 southwestern states (AZ, CA, NM, NV, and UT) decreased from about two million tons per year in 1980 to about one million tons per year in 1991, a change of about 50% (DOE, 1995). Because of prevailing meteorology, emissions in these states are those most likely to influence Grand Canyon visibility.

Analysis of the effects of past changes in emissions on air quality illustrates what previous emissions reductions have accomplished and can provide a yardstick for evaluating the potential effects of future changes. To this end, this section evaluates the particulate sulfur concentration trends at Class I areas on the Colorado Plateau and at other locations in the Southwest and

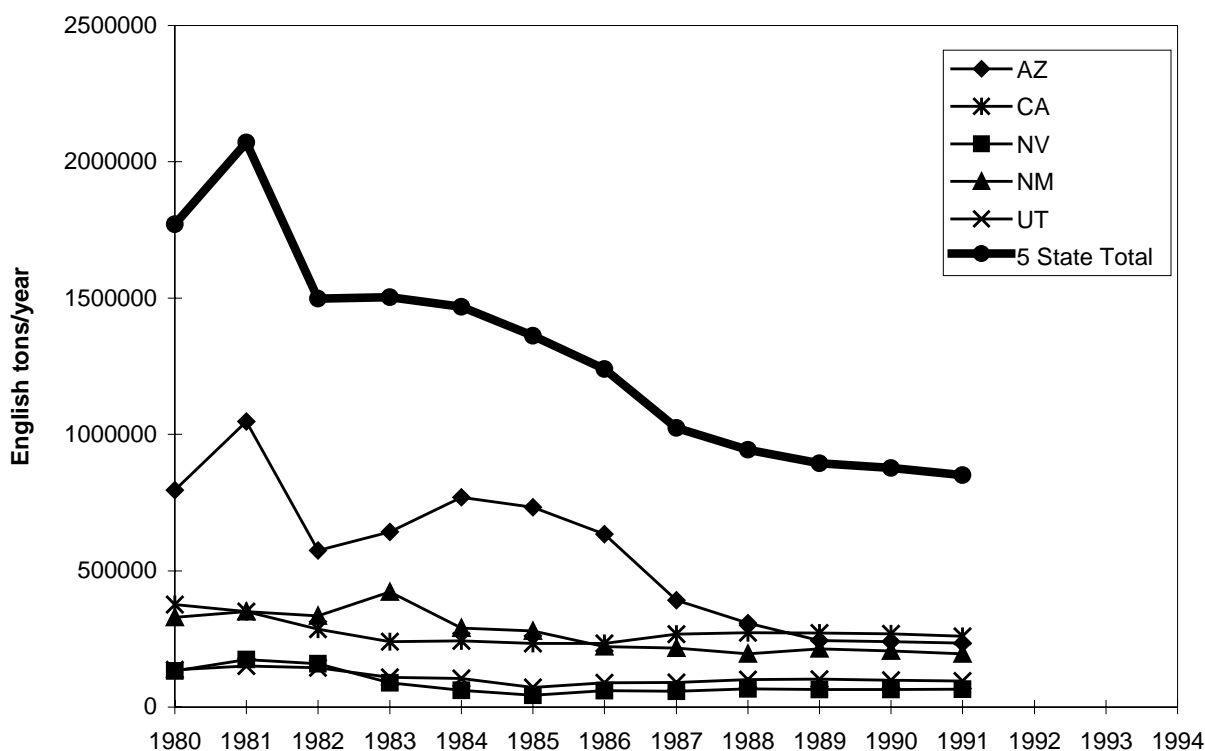


Figure 7-11 Trends in SO<sub>2</sub> emissions in 5 southwestern states.

compares them with the trends in SO<sub>2</sub> emissions in the area. According to Malm *et al.* (1994), sulfate-containing particles accounted for 32% of the average mass of fine particulate matter (PM<sub>2.5</sub>) at Hopi Point in Grand Canyon National Park during the three years 1988-90, and they attributed 35% of the average light extinction due to particles to these same sulfate-containing particles. One might expect that the large decrease in sulfur emissions between 1980 and 1991 would be reflected in ambient particulate sulfur concentration measurements.

### 7.3.1 SO<sub>2</sub> Emissions Trends

The five states whose emissions are plotted on Figure 7-11 are the ones whose emissions are most likely to affect visibility on the Colorado Plateau. In 1991 they accounted for about 60% of the SO<sub>2</sub> emissions in the 11 states of the West. Mexican emissions of SO<sub>2</sub> from sources relatively near the border with the U.S., especially from smelters, grew during this period, but reliable emission trend data are not available.

The emissions trends shown in Figure 7-11 are dominated by the variability in Arizona emissions, which were largely due to smelter operations there. In fact, the large year-to-year variability between 1980 and 1982 reflects a smelter industry strike in 1980 and a very wet El Niño year with low production in 1982. Subsequent decreases during the decade are largely the consequence of shutdowns of several smelters and the installation of emissions control equipment on others. Therefore, the main trend since 1980 has been a strong decline in overall SO<sub>2</sub> emissions in the Southwest, especially in southern Arizona because of smelter emission reductions. Not reflected in this graph is an unquantified increase in Mexican emissions.

### 7.3.2 Particulate Sulfur Trends

Atmospheric concentrations of sulfate or particulate sulfur have been measured since 1979 by the National Park Service (NPS), using two different methods. From 1979 to 1987 the measurements were made in the Western Fine Particle Network (WFPN) with a Stacked Filter Unit (SFU) at a flow rate of 10 l/min for 72 hours (Flocchini *et al.*, 1981). The substrate on which the sample was collected and the area over which it was deposited varied over the years, as indicated in Table 7-1. Since 1987 the aerosol measurements have been performed as part of the IMPROVE program, using multi-unit IMPROVE samplers, at a flow rate of 22.8 l/min for 24 hours (Malm *et al.*, 1994).

*Table 7-1. Chronology of Class I Area Particulate Matter Measurements*

Period	Sampler	Sample Duration	Filter and Sampling Area
7/79 - 5/82	Stacked Filter Unit (SFU)	72 hr	Nuclepore (14 cm <sup>2</sup> )
6/82 - 5/86	Stacked Filter Unit (SFU)	72 hr	Teflon (3.5 cm <sup>2</sup> )
6/86 - 11/87	Stacked Filter Unit (SFU)	24 hr	Teflon (1.1 cm <sup>2</sup> )
3-88 - present	IMPROVE Sampler	24 hr	Teflon (2.2 cm <sup>2</sup> )

Throughout all of the periods listed in Table 7-1, the analysis technique for sulfur in the samples has been the Particle Induced X-ray Emission (PIXE) method, performed by the Crocker Nuclear Laboratory at the University of California at Davis. The PIXE procedure was changed in 1988, when a second detector was added to improve the sensitivity for elements heavier than iron (Eldred & Cahill, 1994). This change improved the precision and minimum detection limits for sulfur, from 8% and 1.9 ng/m<sup>3</sup> in 1982-86 to 5% and 1.4 ng/m<sup>3</sup> from 1988 onward.

Looking at the particulate sulfur measurements, Figure 7-12 shows the behavior of annual average particulate sulfur concentrations at Hopi Point in Grand Canyon National Park and at

three other Colorado Plateau locations for the 15 years from 1980 to 1994. The annual average concentration trend shows a small increase over the 15 years.

When analyzing trends in measured concentrations over periods that include changes in sampling techniques, the possibility that the method changes could have affected the measured concentrations has to be taken into account to assure that a perceived trend does not just reflect a change in the sampling and analysis techniques. The consistency in the annual averages over the 1987 sampler transition seems to suggest that the transition did not cause any significant change in the reported values, but this observation has to be viewed cautiously because the 1987 average does not include the winter season during which the samplers were replaced.

We also confirmed independently that the sulfur concentration trend reflected in Figure 7-12 is not biased greatly by the sampling technique change in 1987 nor by the absence of winter data for 1987, during the transition. We reviewed the sulfur concentrations measured at Hopi Point between 1985 and 1988 by the SCENES cooperative study. SCENES used a different sampler (SCISAS) and the SCENES concentrations during this period were consistently about 10-15% higher than those from the SFU and the IMPROVE sampler. Except for this bias, however, the annual mean sulfur concentrations measured by SCENES closely follow the year-to-year trend

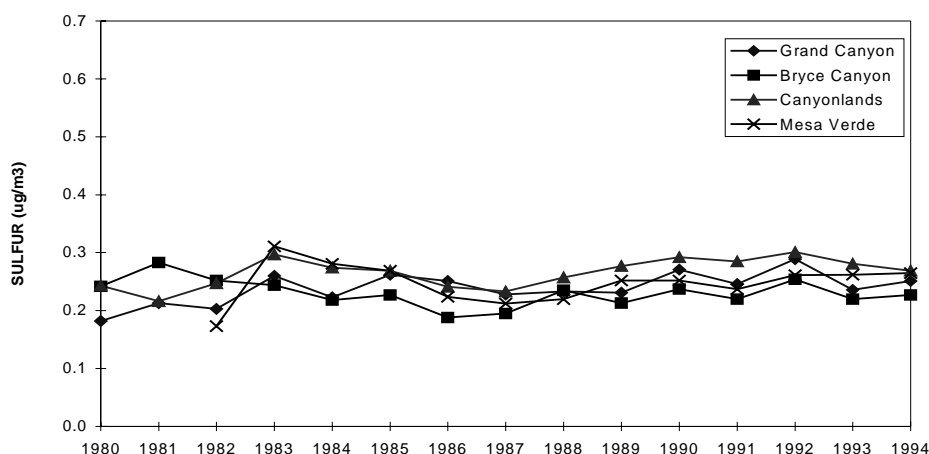


*Figure 7-12 Annual average particulate sulfur concentrations measured by the WFPN and IMPROVE at Hopi Point in Grand Canyon National Park and at three other nearby locations.*

for 1985 to 1989 shown in Figure 7-12 and suggest no introduction of a noticeable change due to the transition.

(One should note that White (1997a) has suggested that the SFU-IMPROVE transition at Shenandoah National Park may have introduced uncertainty into the long-term particulate sulfur trend there. Patterson, *et al.* (1998) argue, however, that such a systematic effect was not observed over the 20 IMPROVE sites they analyzed.)

Thus, despite substantial decreases in SO<sub>2</sub> emissions in the Southwest, we find that a concomitant decrease in particulate sulfur concentrations has not been observed at Hopi Point and at other locations on the Colorado Plateau. In fact, no decrease has been observed at all there.



To explore the reason for this counterintuitive behavior, we analyzed sulfur concentration trends at Class I areas located away from the Colorado Plateau. Figure 7-13 shows the WFPN/IMPROVE annual particulate sulfur concentrations at Big Bend National Park, in southwestern Texas, and at Chiricahua National Monument and Tonto National Forest, both in southern Arizona. The average particulate sulfur concentrations at all three locations are higher than those found at the Colorado Plateau samplers.

Figure 7-13 shows that sulfate concentrations at Big Bend have been increasing since their lowest level in 1984. On the other hand, sulfate concentrations at Tonto and Chiricahua in the 1990's are lower than they were in the early 1980's. (Large year-to-year variability during the WFPN sampling and a 4-year gap in Tonto data introduce some uncertainty to this conclusion, however.)

Eldred and Cahill (1994), also analyzed the same data. They concluded that sulfur concentrations from mid-1982 to mid-1992 decreased at an average rate of 2.7% per year at Mesa Verde and 3.5% per year at Chiricahua. Trends of less than 0.6% per year (either increase or decrease), which is less than the standard error of the estimates, were found at Big Bend, Bryce Canyon, Canyonlands, and Grand Canyon. Their statistical findings are consistent with the results presented here.

We can conjecture about the reasons for the observed behavior. The largest SO<sub>2</sub> emissions reductions took place at the smelters in southern Arizona, a region from which transport infrequently reaches the Colorado Plateau except during late summer monsoons. Therefore, these emission reductions had little effect on annual average sulfate concentrations on the Colorado Plateau. At locations in southern Arizona (Tonto and Chiricahua), however, the effects of the more nearby smelter emission changes were noticed, including effects of the strike in 1980, the wet year in 1982, and permanent shutdowns of two smelters in 1985.

During this same period (mid 1980's), the Nacozari smelter entered service in Mexico. This smelter location is far enough south and east of the Tonto and Chiricahua Class I areas that its emissions don't affect the air quality at those locations frequently. Rather, the generally westerly flow carries its emissions toward Big Bend National Park, where the sulfate concentrations shown in Figure 7-13 appear to reflect both the U.S. smelter emissions reductions in the early 1980's and subsequent increases in Mexican emissions since then, from smelters and other sources.

The above analyses have addressed trends in particulate sulfur concentrations. A similar attempt to discern a trend in total PM<sub>2.5</sub> mass concentrations was not successful, however, because it was found that the IMPROVE determinations of gravimetric mass concentrations are larger than those measured by the SFU.

The analyses above have demonstrated that trends in particulate sulfur concentrations on the Colorado Plateau from 1980 to 1994 have been weak despite substantial decreases in regional SO<sub>2</sub> emissions. Receptors to the south, in the vicinity of the smelters that have produced most of the emission reductions, have shown some decrease in sulfate particle concentrations, although the average change has been less than the reduction in emissions. Thus, it appears that the average Colorado Plateau air quality has been relatively detached from the SO<sub>2</sub> emissions

changes. This does not mean, though, that emissions changes in southern Arizona and northern Mexico will not affect Colorado Plateau air quality occasionally.

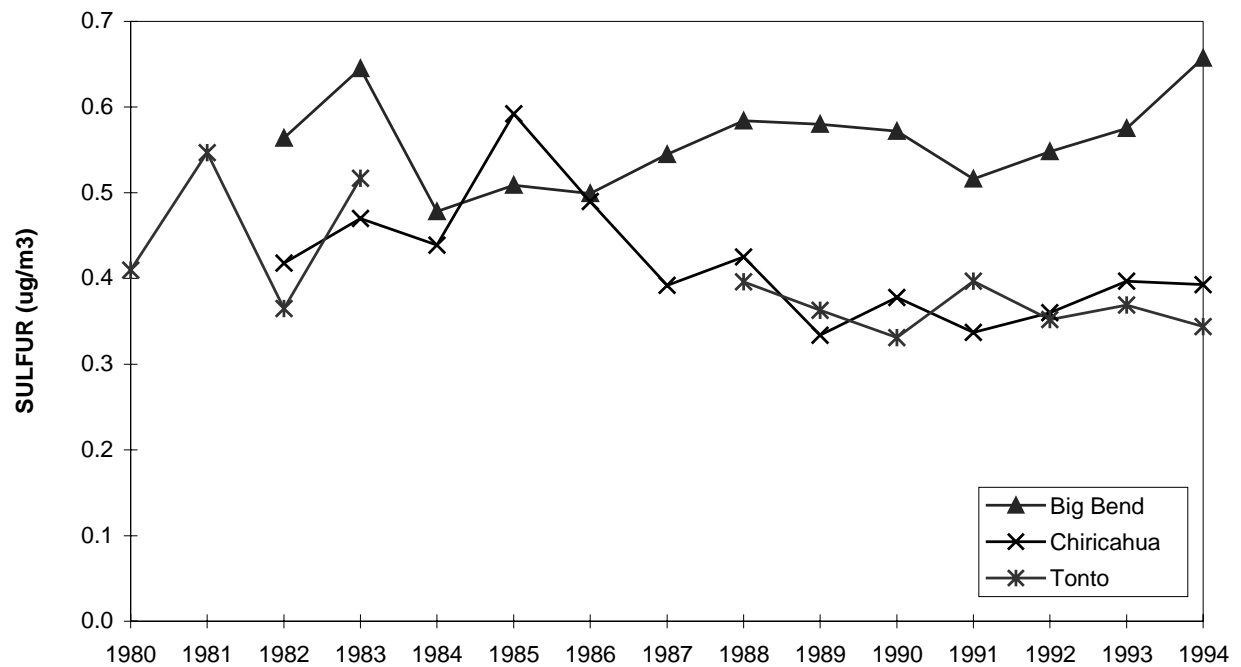


*Figure 7-13 Annual average particulate sulfur concentrations measured by the WFPN and IMPROVE at three locations away from the Colorado Plateau.*